Temperature-Dependent Two-State Dynamics of Individual Cooperatively Rearranging Regions on a Glass Surface

S. Ashtekar, J. Lyding, and M. Gruebele

Phys. Rev. Lett. **109**, 166103 — Published 19 October 2012

DOI: 10.1103/PhysRevLett.109.166103

Temperature-dependent two-state dynamics of individual cooperatively rearranging regions on a glass surface

S. Ashtekar,[1,2] J. Lyding[1,3] and M. Gruebele[1,2,4]

[1]Beckman Institute for Advanced Science and Technology, [2]Department of Chemistry. [3]Department of Electrical and Computer Engineering, and [4]Department of Physics, University of Illinois, Urbana, IL 61801 USA.

(Received)

PACS numbers: 68.37.Ef, 68.35.bj, 63.50.Lm, 64.70.pe, 81.05.Kf

Cooperatively rearranging regions (CRRs) play a central role in the temperature dependence of glass dynamics. We record real-time atomic resolution movies of individual CRRs, while ramping their temperature. Between 295 and 326 K, well below the bulk glass transition temperature T_g, the rate coefficient for two-state hopping of CRRs increases over 10-fold, yielding an Arrhenius activation barrier of $\approx 10\ k_B T_g$. By time-resolving the dynamics of many individual CRRs, we show that highly stretched dynamics of the CRR ensemble results mainly from spatial heterogeneity, less from temporal heterogeneity of individual CRRs.

As a glass forms, units such as atoms, molecules, polymers, or colloids become locked together into cooperatively rearranging regions (CRRs) on ever-increasing length scales [1-3]. The units in a CRR move collectively, resulting in very slow dynamics below the glass transition temperature T_g. There has been much experimental progress in studying the heterogeneous dynamics of CRRs. Measurements ranging from anomalous low-temperature frequency response [4], to 'telegraph style' dynamics [5, 6] have shown that CRRs exhibit two-state or at most few-state dynamics below T_g. The size of CRRs is a few diameters of the glass forming unit [7], based on relating the measured dynamical susceptibility to spatial correlations [8], and more directly via scanning probe microscopy of a few CRRs [5], or imaging of individual CRRs [9]. In better aged (lower enthalpy) glasses, CRRs are thought to be larger [1].

Observing the motion of individual CRRs with atomic resolution as a function of temperature could reveal unambiguous information about the underlying energy landscape of glasses. Currently the activation enthalpy of CRRs on atomic glass surfaces has been determined only indirectly by assuming a rate prefactor [9]. The atomic sub-structure of CRRs has not been resolved. The origin of heterogeneous dynamics of the CRR ensemble could be mainly inhomogeneous (different CRRs behave differently), or it could be mainly homogeneous (individual CRRs behave differently with time because of changes in their environment). It is also possible that these two effects could make similar contributions, depending on the time scale of the observations.

We present measurements that resolve these issues for CRRs at an atomic glass surface. We imaged individual CRRs at metallic glass surfaces while ramping their temperature, obtaining real-time movies of their temperature-dependent dynamics. We studied a $Fe_{78}B_{13}Si_8$ alloy (as-received 25.4 μm thick MetGlas® SA1 samples from MetGlas Inc., Conway SC, USA) with a glass transition temperature of T_g = 780 K. Samples were degassed for 8 hours at 373 K and cleaned using 2 keV argon ion sputtering with a dose of ~1 to 10×10^{16} ions/cm^2. The surface composition analyzed by X-ray photoelectron spectroscopy was very similar to the bulk. Oxide-free samples were transferred directly from the sputtering chamber into a home-built ultra-high vacuum scanning tunneling microscope (P $<1.3 \times 10^{-9}$ Pa) [10], and scanned with electrochemically etched tungsten probe tips. To observe samples at the highest resolution, 1-2 V sample bias and 10 pA tunneling currents were employed. As shown previously, currents up to 100 pA produce no appreciable acceleration of observed dynamics due to surface heating (ref. [9], see its Fig. S1). STM movies with a time resolution of 1.3 to 6 minutes per frame were recorded for up to 1000 minutes at variable temperature. Image size was 25×25 nm^2, and spatial autocorrelation was used to overlap successive frames before truncating the movies to an area common to all images. A custom-built heater newly integrated into the scanning platform provides I^2R heating up to 440 K and in-situ temperature monitoring for temperature-ramping measurements, as long as the ramp is tuned slowly enough so the tip can retract while maintaining imaging.

CRRs imaged at atomic resolution have irregular but compact (aspect ratio ≤ 1:2) surfaces capped by 5-8 alloy atoms. Atomic resolution reveals that upon hopping between configurations, the CRR shape reorganizes on a length scale not more than 1 atom (≈0.3 nm;

Figure 1ab). CRRs hop mainly between two states (structurally distinct configurations), as observed previously [9]. The <6% of mobile CRRs that make transitions between more configurations hop among pairs or sequential triplets of configurations. One such CRR, imaged at atomic resolution, is shown in Fig. 1a. The time trace in Fig. 1c reveals that three configurations are visited, and can only interconvert as 0→1→2→0 on the time scale of our measurement.

We were able to monitor individual CRRs while ramping their temperature. In Figure 2, only a single CRR initially moved (full movie in SI). When the temperature was ramped from 323 to 326 K, two additional clusters began to hop between two configurations. Thus CRR hopping is a thermally activated process. Increasing the temperature obviously facilitates barrier crossing, but it could also change the stability of different CRR configurations on the energy landscape. We were able to quantitatively measure both effects.

Changes of the energy landscape were monitored by collecting many CRR time traces (see Fig. S2 and movie in SI). An example of a trace with activity both before and after a temperature ramp is shown in Fig. 3a, with dwell times in the two states labeled t_0 and t_1. In this particular example, the average relaxation rate given by $\langle k_{obs} \rangle = \langle 1/t_0 + 1/t_1 \rangle$ does not change upon heating, but the equilibrium population ratio $K_{eq} = \langle t_1 \rangle / \langle t_0 \rangle$ of the two configurations shifts heavily in favor of state 1 after the temperature is ramped up. Figure 3b shows quantitatively how the energy landscape has shifted in terms of a double-well potential (see eq. (1) for model).

The sequence of dwell times before and after a temperature ramp may or may not correspond to the same values of k_{obs} and K_{eq}. To decide whether the observed change in CRR activity was due to a change in k_{obs} and/or K_{eq} or just coincidence, we compared all time traces with a Kolmogorov-Smirnov test [11]. For each experimental trace, the input for this test consisted of multiple simulated Markov traces, down-sampled to the STM scan rate and matching the length and average k_{obs} and K_{eq} of the experimental trace. The result of this test is two probability distributions of k_{obs} and K_{eq} for the two traces being compared, and a probability p that these two distributions are identical (see SI for more details). Fig. 3c shows the probability distributions $P(-\ln[K_{eq}], -\ln[k_{obs}])$ before and after the temperature ramp. The distributions indicate a clear shift of the energy landscape, but not of the rate, in this particular case. The Kolmogorov-Smirnov likelihood that the two probability distributions are accidentally the same is $p = 0.03$.

Averaged over all CRRs, we found a large and significant increase of the two-state relaxation rate with temperature. The average rate coefficient increased from $<k_{obs}>$=0.066 min^{-1} at 295 K to 0.575 min^{-1} at 323 K. Our movies have a finite time resolution; therefore some hopping transitions are missed while the STM tip is not scanning over a CRR. To correct for this aliasing effect, we calculated prior dwell time distributions by simulating an ensemble of traces with the kinetic model of eq. (1), which, when down-sampled, matched the experimentally observed of $<t_0>$ and $<t_1>$. The corrected rate coefficients of 0.080 and 0.863 min^{-1} yielded a similar ratio of rate coefficients as the raw data. We used these values to estimate the average activation barrier from the Arrhenius equation with constant prefactor A and energies defined in Fig. 3b:

$$k_{obs}(T) = Ae^{-E_{surf}/k_BT}\,2\cosh(\Delta E/2k_BT), \quad K_{eq}(T) = e^{-\Delta E/k_BT}. \qquad (1)$$

The result is E_{surf} = 9.5 k_BT_g for the raw data, and E_{surf} = 10.4 k_BT_g for the aliasing-corrected data. From this we deduce a prefactor A in the range of $6\cdot10^9$ s^{-1} to $6\cdot10^{10}$ s^{-1} (see SI for details beyond eq. (1)). The upper end of this range is consistent with barrier-free hopping times of a ~5^3 atom cluster of mass m ~7 kDa over a distance of Δx~2 nm at room temperature (Δt~[$m\Delta x^2/k_BT$]$^{1/2}$).

For the metallic glass surface, we can meaningfully distinguish spatial heterogeneity among multiple CRRs from temporal heterogeneity of individual CRRs. To do so, we scaled t_0 and t_1 dwell times separately for each individual cluster to a unitless average $<t_{dwell}>$ = 1, then produced a histogram of the dwell time distribution. This scaling removes CRR-to-CRR spatial heterogeneity from the dwell times. To simulate the ensemble average for comparison, we simply created a histogram of all dwell times and then scaled the average dwell time to 1. The two plots are shown in Fig. 4, comparing both raw and aliasing-corrected data. The results from the raw and aliasing-corrected data are again very similar. The individually normalized dwell time distribution is well fitted by a single exponential dwell time distribution (a stretched exponential fit to exp[-t$^{\beta}$] yielded β=1.1±0.2; see Fig. S3). In contrast, the ensemble histogram is well represented by a power law ~$(a+t_{dwell}/\delta)^{-\delta}$ with exponent δ=2 (a stretched exponential fit was not satisfactory; see Fig. S3).

A power law is characteristic of a particularly wide distribution of dwell times. The dwell time distributions $\psi(t_{dwell})$ in Fig. 4 are related directly to the ensemble relaxation signal $G_{1\leftarrow0}(t)$ and to the distribution of rate coefficients via Laplace transforms [12]. While the exponential fit

to the individual CRR dwell time distribution in Fig. 4A corresponds to a single rate coefficient and single exponential (Markovian) relaxation dynamics, the power law for the ensemble in Fig. 4B corresponds approximately to a power law distribution of rate coefficients, in agreement with recent predictions [17] of very broad distributions of rate coefficients for α relaxations in glasses.

The majority of ensemble behavior clearly arises from spatial heterogeneity of rates among different clusters. This is not to say that individual CRRs do not exhibit temporally fluctuating kinetics when other CRRs' dynamics alters their local energy landscape. For example, the cluster in the bottom left frame of Fig. S1 'stalls' for a while in the middle of the trace. The Kolmogorov-Smirnov test applied to such time segments yields a significant probability that the underlying rate coefficient was time-dependent for that cluster. As discussed by Kaufman and coworkers, temporal heterogeneity of individual clusters may be greater on time scales outside our dynamic range of a few hours [13] spanned by our data. Near the bulk glass transition T_g, kinetically facilitated models do not predict such a neat partitioning into CRR-to-CRR vs. individual CRR heterogeneity [14]; it would be interesting to see what such models predict deep within the glassy regime, where our observations are made.

Our direct imaging of CRRs at variable temperature can be compared with polymer, colloid, or more indirect measurements on molecular glasses. For a molecular glass with similar-sized units (glycerol) as our metallic glass, Berthier *et al.* were able to deduce a diameter of CRRs, $\xi \sim$ 0.9 to 1.5 nm from 232 to 192 K. We imaged a 0.5 to 2 nm distribution, with a temperature dependence between 295 and 323 K significantly smaller than the distribution width of ±0.75 nm. The size range of clusters exceeds the largest size variation (ξ~0.3 nm) we observed among the two configurations occupied by an individual CRR. Like Russell *et al*., we were able to observe 'telegraph style' traces with stretched kinetics, and our imaging reveals their origin: spatial heterogeneity of the ensemble average, whereas individual clusters obey mainly exponential kinetics on a time scale < 1 hr. On longer time scales, individual CRR hopping rates may fluctuate, and we see statistically significant fluctuations (again by Kolmogorov Smirnov test) in some members of our observed ensemble.

Reorganization of the glass surface is not necessarily the same as in the bulk, or as in thin films. CRRs have more freedom to move around obstacles on a surface. The surface CRRs we observe share features of both α or β relaxations used to describe the bulk. On the one hand, their shape is compact. This agrees with predictions of compact rather than 'stringy' shapes [15]

at low temperature, and our measurements are well below the bulk $T_g \approx 780$ K. On the other hand, our barrier (~10 $k_B T_g$) deduced from the Arrhenius law is rather small for an α relaxation. Surface-specific glass models predict more facile α reorganization than in the bulk (~18 $k_B T_g$) [16], although our observed barriers are yet somewhat smaller. However, when the configurational entropy per atom exceeds 1 k_B [15] [17], models predict a continuous distribution of activation energies over the range conventionally labeled "β" (fast, localized dynamics) to "α" (slow, collective dynamics), which has a broad peaked near 10 $k_B T_g$ with a tail towards higher barriers (Fig. 4C). Our observed distribution of barrier heights at 295 K is peaked at ~ 10 $k_B T_g$ with a tail towards higher barriers (Fig. 4C). A quantitative comparison with theory cannot be made yet because our current experimental dynamic range is too small; it is possible that our experiment misses a tail of large barriers that would require > 1 day observation times, or small barriers that result in hops < 1 minute.

Fast dynamics of surface glasses raises an interesting question for future investigation: to what extent are T_g the same in the bulk and near the surface? Work by Fakhraii *et al.*[18], and Daley *et al.* [19] already illustrates the special nature of surface glass dynamics. They probed surface *vs.* bulk diffusion of gold nanoparticles in and on glasses. Thin glass films prepared near T_g by vapor deposition are able to settle much lower on the free energy landscape due to better surface mobility, approaching the limiting Kauzmann entropy [20, 21]. The surface is effectively much more 'aged' than the bulk. Based on our observations, we expect that metallic glass surfaces will have a higher T_g than their bulk phase, and may even turn out to be 'indestructible' (not re-crystallizable) in some materials.

Acknowledgments

This work was funded by support from the Eiszner family (James R. Eiszner Chair), and NSF grant CHE 0948382. S.A. was recipient of a Beckman Graduate Fellowship while carrying out this work.

References

[1] E. Donth, *The glass transition* (Springer, Berlin, 2001), p. 418.
[2] G. Adam, and J. H. Gibbs, J. Chem. Phys. **43**, 139 (1965).
[3] V. Lubchenko, and P. G. Wolynes, Ann. Rev. Phys. Chem. **58**, 235 (2007).
[4] X. Liu *et al.*, Phys. Rev. Lett. **78**, 4418 (1997).
[5] E. V. Russell, and N. E. Israeloff, Nature **408**, 695 (2000).
[6] S. Ashtekar *et al.*, Physical Review Letters **106**, 235501 (2011).
[7] U. Tracht *et al.*, Physical Review Letters **81**, 2727 (1998).
[8] L. Berthier *et al.*, Science **310**, 1797 (2005).
[9] S. Ashtekar *et al.*, J. Phys. Chem. Lett. **1**, 1941 (2010).
[10] P. M. Albrecht, and J. W. Lyding, Small **3**, 146 (2007).
[11] J. A. Peacock, Monthly Notices of the Royal Astronomical Society **202**, 615 (1983).
[12] M. Boguñá, A. M. Berezhkovskii, and G. H. Weiss, Physica A **282**, 475 (2000).
[13] S. A. Mackowiak, and L. J. Kaufman, J. Phys. Chem. Lett. **2**, 438 (2011).
[14] F. Ritort, and P. Sollich, Adv. in Phys. **52**, 219 (2003).
[15] J. D. Stevenson, J. Schmalian, and P. G. Wolynes, Nature Physics **2**, 268 (2006).
[16] J. D. Stevenson, and P. G. Wolynes, J. Chem. Phys. **129**, 234514 (2008).
[17] J. D. Stevenson, and P. G. Wolynes, Nature Physics **6**, 62 (2010).
[18] Z. Fakhraai, and J. A. Forrest, Science **319**, 600 (2008).
[19] C. R. Daley *et al.*, Soft Matter **8**, 2206 (2012).
[20] M. D. Ediger, C. A. Angell, and S. R. Nagel, J. Phys. Chem. **100**, 13200 (1996).
[21] W. Kauzmann, Chem. Rev. **43**, 219 (1948).

Figure Captions

Fig. 1 Internal structure of a CRR. **a** shows the three distinct states (0, 1, and 2) a CRR displays at 295 K, while a red trace outlines the periphery of the CRR in each state. **b** shows the dimensions for some internal structures of each state. Scale bar = 0.71 nm (3 average atomic diameters). **c** shows the full time trace of this CRR illustrating the connectivity between the states as '1→2→0→1⋯'.

Fig. 2 Temperature-resolved dynamics of individual CRRs. Still from a movie (see SI) where the metallic glass surface is imaged with nm-resolution while simultaneously increasing the temperature by 3 K. Three colored arrows point towards the three CRRs of interest, all exhibiting two-state motion. The color-coded time traces show their dynamics, while the black dot traces their position as the movie progress. Two cluster traces (2nd and 3rd in the figure) show increased activity when the temperature ramp starts.

Fig. 3 Temperature-sensitive energy-landscape. **a** A variable temperature time trace starting at 323 K, followed by a brief temperature ramp to 325.5 K, then isothermal again. A dwell time in state '0' is labeled t_0, another in state '1' t_1. Before the ramp, $k_{obs} \approx 0.79$ min^{-1}, $K_{eq} \approx 1$, after the ramp $k_{obs} \approx 0.79$ min^{-1}, $K_{eq} \approx 16.8$. **b** depicts the two-state free energy wells in $k_B T_g$ units before and after the ramp, which stabilizes state '1'. **c** shows the probability distributions of rate coefficients (A is defined in eq. 1) and equilibrium population ratios of the cluster in the initial (blue) and the final (red) part of the trace. The Kolmogorov-Smirnov test indicates that the likelihood these two distributions came from a single underlying joint distribution is low (p = 0.03).

Fig 4 Spatial heterogeneity leads to non-exponential kinetics. **a** Dwell time histograms of 25 two-state CRRs recorded at 295 K (see Fig S1 for all cluster traces). Open circles: dwell times t_0 and t_1 are scaled for each cluster individually so their average equals 1, then histogrammed; the average of the t_0 and t_1 histograms is shown. Solid squares: histogram corrected for aliasing due to a finite STM sampling rate. The solid line shows a fit to the exponential Aexp(-t), depicting nearly exponential kinetics of individual clusters. **b** Same histogram, but with all times

histogrammed first and then scaled to an average of 1, corresponding to ensemble kinetics. Spatial heterogeneity from CRR to CRR causes slower decay of dwell time probability best fit to a power law (δ =2). See SI for separate t_0 and t_1 histograms and histograms of 323 K data. **c** Solid: experimental distribution of rate coefficients k_{obs} for the same clusters, converted to barrier heights using eq. (1). Dotted: theoretical bulk barrier distribution from ref. [17] for configurational entropy $s_C = 1\ k_B T_g$. The experiment's dynamic range (1 min to several hours) is limited, and may sample only a sliver of the actual barrier distribution.

Fig 1

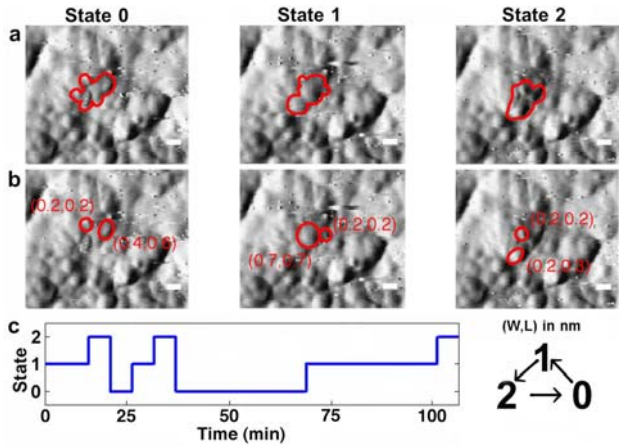
State 0
State 1
State 2
a
b
(0.2,0.2)
(0.4,0.6)
(0.2,0.2)
(0.7,0.7)
(0.2,0.2)
(0.2,0.8)
c
State
2
1
0
0
25
50
75
100
Time (min)
(W,L) in nm
1
2
0

Fig 2

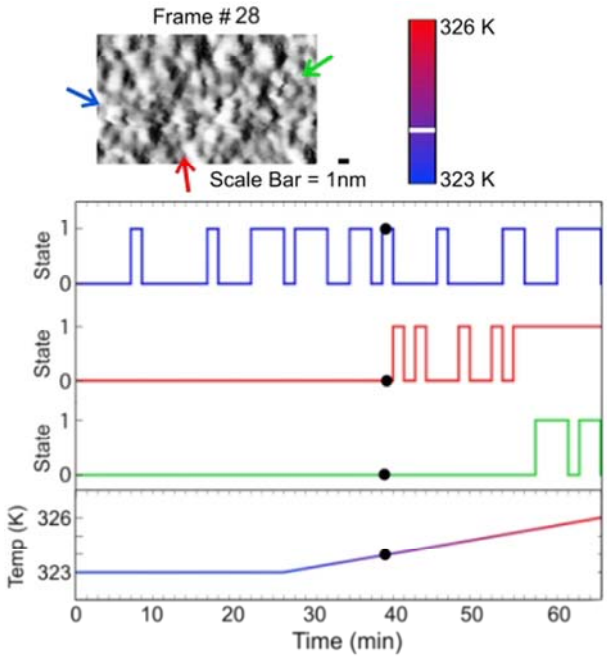
Frame # 28
326 K
323 K
Scale Bar = 1nm
State
1
0
State
1
0
State
1
0
Temp (K)
326
323
0
10
20
30
40
50
60
Time (min)

Fig 3

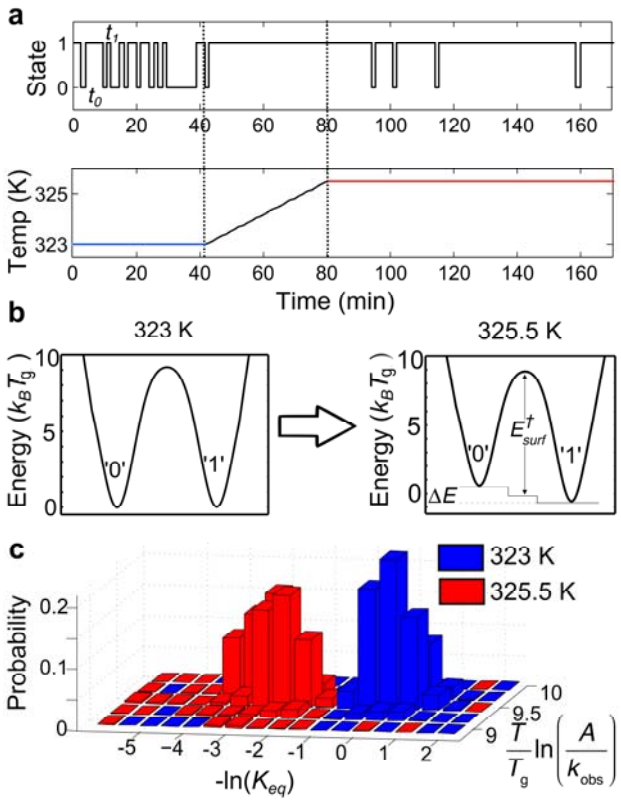
a
State
1
0
t_1
t_0
0 20 40 60 80 100 120 140 160
Temp (K)
325
323
0 20 40 60 80 100 120 140 160
Time (min)
b
323 K
325.5 K
Energy ($k_B T_g$)
10
5
0
'0'
'1'
$E^{\dagger}_{surf}$
ΔE
c
323 K
325.5 K
Probability
0.2
0.1
0
-5 -4 -3 -2 -1 0 1 2
-ln(K_{eq})
10
9.5
9
$\frac{T}{T_g} \ln\left(\frac{A}{k_{obs}}\right)$

Fig 4

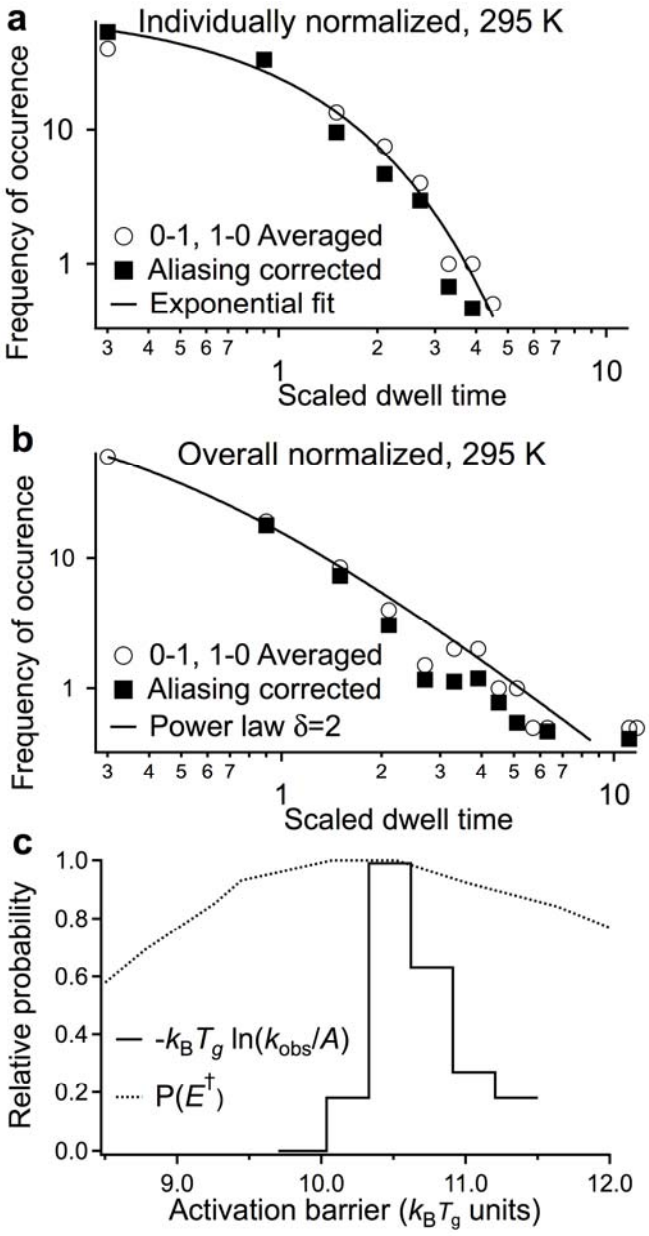
a
Individually normalized, 295 K
Frequency of occurence
10
1
○ 0-1, 1-0 Averaged
■ Aliasing corrected
— Exponential fit
3 4 5 6 7
1
2 3 4 5 6 7
10
Scaled dwell time
b
Overall normalized, 295 K
Frequency of occurence
10
1
○ 0-1, 1-0 Averaged
■ Aliasing corrected
— Power law δ=2
3 4 5 6 7
1
2 3 4 5 6 7
10
Scaled dwell time
c
Relative probability
1.0
0.8
0.6
0.4
0.2
0.0
— $-k_B T_g \ln(k_{obs}/A)$
····· $P(E^{\dagger})$
9.0
10.0
11.0
12.0
Activation barrier ($k_B T_g$ units)